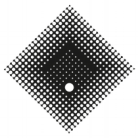

Fractional and fractal derivative-based creep models for concrete under constant and time-varying loading

Fractional and fractal derivative-based creep models for concrete under constant and time-varying loading

Y. Bouras*and Z. Vrcelj

College of Engineering and Science, Institute of Sustainable Industries and Liveable Cities, Victoria University, 3011, Melbourne, Australia

Emails: yanni.bouras@vu.edu.au, zora.vrcelj@vu.edu.au

*Corresponding author

Abstract. *In this paper, fractional and fractal derivative-based viscoelastic laws are adopted to develop linear creep models for reinforced and prestressed concrete under constant and time-varying loading. The model parameters are determined by curve-fitting the creep compliances of the spingpot and Kelvin-Voigt viscoelastic models to experimental data of basic creep in plain concrete specimens. Equilibrium and strain compatibility equations are formulated for reinforced and prestressed concrete under concentric loading which are solved simultaneously with the constitutive stress-strain equation of the selected viscoelastic model. For the case of a constant load, adoption of the fractal viscoelastic models lead to first-order differential equations that, when solved, yield analytical expressions for basic creep in reinforced and prestressed concrete. A semi-analytical solution is derived when adopting the fractional viscoelastic laws, obtained using the Laplace transform technique. Both models ensure strain compatibility and consider stress redistribution from concrete to the steel reinforcement bars. A high-level of agreement is made between the derived fractional and fractal-derivative based models and existing experimental data of creep in reinforced and pre-stressed concrete members under constant load. When the applied loading varies with time, numerical procedures are employed to approximate the fractional and fractal derivatives. It is found that creep in plain concrete members subjected to time-varying loads is accurately predicted when using the fractional derivative models. Comparisons are then made to other methods of modelling creep under time-varying stress. The primary advantage of the derived models is that only up to three parameters require calibration using basic creep tests for an accurate representation of creep and that closed-form expressions for creep can be obtained for the case of constant, sustained loading.*

Keywords: Creep; Fractal derivative; Fractional derivative; Reinforced concrete; Viscoelasticity;

1 Introduction

Viscoelastic materials can be defined as exhibiting both viscous and elastic properties during deformation. Traditional viscoelastic models, including the Maxwell, Kelvin-Voigt (KV), Zener and anti-Zener (AZ) models, consist of an arrangement of elastic springs and dashpots (D) in series and/or parallel. Despite their common adoption, these models cannot accurately describe the dynamic behavior of real materials [1]. High levels of accuracy can be obtained when viscoelastic chains are employed to describe material behavior. However, the required multitude of viscoelastic elements results in a great number of material parameters to be characterized which can convolute analytical and numerical modelling [2].

The traditional models of viscoelasticity can be generalized by replacing the integer-order derivative in the constitutive stress-strain relation by a fractional or real order, resulting in the models of fractional viscoelasticity [3] . The study of performing integration and differentiation to a non-integer order is called Fractional Calculus [4]. Many definitions of the fractional derivative have been proposed including the Reimann-Liouville and Caputo. The left-sided

Riemann-Liouville fractional integral of a function $f(t)$ of order $\alpha > 0$ where $\alpha \in R^+$ is defined as;

$$D_t^{-\alpha} f(t) = \frac{1}{\Gamma(\alpha)} \int_0^t (t-\tau)^{\alpha-1} f(\tau)\ d\tau, \tag{1}$$

and the left-sided Riemann-Liouville fractional derivative of a function $f(t)$ of order $0 < \alpha < 1$ is known as;

$$D_t^{\alpha} f(t) = \frac{1}{\Gamma(1-\alpha)} D_t^1 \int_0^t \frac{f(\tau)}{(t-\tau)^{\alpha}}\ d\tau. \tag{2}$$

In Eqs. (1) and (2), Γ denotes the Gamma function;

$$\Gamma(\alpha) = \int_0^{\infty} e^{-t} t^{\alpha-1}\ dt. \tag{3}$$

The stress-strain relations and creep compliances of the fractional dashpot (FD), fractional Kelvin-Voigt (FKV) and fractional anti-Zener (AZ) models of viscoelasticity are listed in Table 1 in addition to their traditional counterparts. In Table 1, η is the dynamic viscosity of the springpots (fractional dashpots) in the D and KV models, E is the modulus of elasticity of the spring in the rheological models, η_1 and η_2 denote the dynamic viscosity of the first and second springpots in the AZ model respectively, and $D_t^x(\ )$ is the operator of differentiation of order x. Note that the order of differentiation $0 < \alpha < 1$ in the constitutive stress-strain equations of the fractional viscoelastic models. The mechanical analogues of these rheological models are depicted in Fig. 1. Researchers have shown that fractional viscoelasticity is an effective method of modelling time-dependent behaviour of rocks and soils [5-8] and creep behavior of concrete. Bouras et al. [9] developed a thermo-viscoelastic rheological model based on fractional derivatives to describe creep in plain concrete at extreme temperatures. The analysis was limited to the sprinpot model of viscoelasticity and accuracy of the develop model at ambient temperature was low. Paola and Granata [10] proposed a fractional viscoelastic model for the hereditary behaviour of concrete. Ageing effects were considered by calibrating the fractional order and dynamic viscosity of the springpot model of viscoelasticity at different loading ages. The same approach was adopted by Beltempo et al. [11], where a fractional-order creep function was proposed for aging concrete by fitting the springpot model parameters to the B3 concrete creep model at various initial loading times. Though these works considered ageing effects through loading time, the effect of time-varying stresses on creep was not analysed. Zhang et al. [12] developed a nonlinear creep damage constitutive model for plain concrete under high stress using a fractional viscoelastic springpot. Overall, the power-law form of the memory kernels in fractional viscoelastic models allow highly accurate representations of experimental data with the benefit of few model parameters requiring characterization [13]. Additionally, fractional viscoelastic laws feature a full reciprocal relationship between creep and stress relaxation laws. This allows stress relaxation curves to be obtained using the same model parameters from the creep compliance, which is convenient as experimental creep tests are commonly conducted [10]. The mathematical consistency also gives application to the Boltzmann superposition principle for analysis of the effects of time-varying stresses and strains. However, when model parameters and applied stress vary with time, numerical approximations must be employed to solve fractional equations which are dependent on strain history leading to an increase of computational costs.

The large computational requirements associated with solving fractional derivatives can be avoided using fractal derivatives, which were derived as a local derivative to model the complex behaviour of fractal materials. The fractal derivative of a function $f(t)$ of order p is defined as;

$$D_t^p(f) = \frac{D_t^1(f)}{p \times t^{p-1}}, \tag{4}$$

where fractal order $p > 0$. Cai et al. [14] first employed fractal derivatives to characterise viscoelastic materials and proposed the fractal M and fractal KV viscoelastic models by replacing the integer-order derivative in the constitutive equations with a fractal order. Table 1 provides the stress-strain constitute relations and corresponding creep compliances of the fractal M, fractal KV and fractal AZ models where $0 < p < 1$. It shown that the creep compliances of the fractal models can be obtained by replacing time t in the traditional creep compliances with t^p [14]. As with fractional viscoelastic models, fractal models are more accurate than the traditional M and KV models whilst featuring fewer model parameters. However, fractal models were found to be computationally more efficient than fractional models whilst featuring simpler mathematical expression and yielding similar accuracy. Despite the evident advantages of modeling viscoelastic materials with fractal derivatives, adoption in civil engineering applications is limited. Wang et al. [15] developed a fractal derivative-based viscoelastic model considering damage evolution to describe the trimodal creep behaviour of granite, and Qu et al. [16] simulated chloride diffusion in fly-ash concrete using fractal and fractional derivatives.

Table 1 Governing equations of traditional, fractional and fractal viscoelastic models

Model	Stress-strain relation	Creep compliance $J(t)$
D	$D_t^1(\epsilon_{cr}) = \frac{\sigma}{\eta}$	$\frac{t}{\eta}$
KV	$D_t^1(\epsilon_{cr}) + \frac{E}{\eta}\epsilon_{cr} = \frac{\sigma}{\eta}$	$\frac{1}{E}\left(1 - e^{Et/\eta}\right)$
AZ	$\sigma + \left(\frac{\eta_1 + \eta_2}{E}\right) D_t^1(\sigma) = \eta_2 D_t^1(\epsilon_{cr}) + \left(\frac{\eta_1\eta_2}{E}\right) D_t^2(\epsilon_{cr})$	$\frac{1}{E}\left(1 - e^{Et/\eta_1}\right) + \frac{t}{\eta_2}$
FD	$D_t^\alpha(\epsilon_{cr}) = \frac{\sigma}{\eta}$	$\frac{t^\alpha}{\eta \times \Gamma(1+\alpha)}$
FKV	$D_t^\alpha(\epsilon_{cr}) + \frac{E}{\eta}\epsilon_{cr} = \frac{\sigma}{\eta}$	$\frac{1}{E}\left[1 - \mathcal{E}_\alpha\left(-\frac{E}{\eta}t^\alpha\right)\right]$
FAZ	$\sigma + \left(\frac{\eta_1 + \eta_2}{E}\right) D_t^\alpha(\sigma) = \eta_2 D_t^\alpha(\epsilon_{cr}) + \left(\frac{\eta_1\eta_2}{E}\right) D_t^{1+\alpha}(\epsilon_{cr})$	$\frac{1}{E}\left[1 - \mathcal{E}_\alpha\left(-\frac{E}{\eta_1}t^\alpha\right)\right] + \frac{t^\alpha}{\eta_2 \times \Gamma(1+\alpha)}$
Fractal D	$\frac{D_t^1(\epsilon_{cr})}{p \times t^{p-1}} = \frac{\sigma}{\eta}$	$\frac{t^p}{\eta}$
Fractal KV	$\frac{D_t^1(\epsilon_{cr})}{p \times t^{p-1}} + \frac{E}{\eta}\epsilon_{cr} = \frac{\sigma}{\eta}$	$\frac{1}{E}\left(1 - e^{Et^p/\eta}\right)$
Fractal AZ	$\sigma + \frac{(\eta_1 + \eta_2) D_t^p(\sigma)}{Ept^{p-1}} = \eta_2 D_t^p(\epsilon_{cr}) + \frac{\eta_1\eta_2 D_t^{1+p}(\epsilon_{cr})}{Ept^p}$	$\frac{1}{E}\left(1 - e^{Et^p/\eta_1}\right) + \frac{t^p}{\eta_2}$

In this paper, fractional and fractal viscoelastic laws are utilised for the development of creep models for reinforced and prestressed concrete under constant and time-varying loading. There is no available research in the open literature that utilizes fractal viscoelasticity theory for concrete creep modelling, and studies on fractional viscoelasticity rarely consider time-varying stresses and the effects of reinforcement on creep. This research seeks to address these limitations with the literature and aims to derive a robust concrete creep model that captures the advantages of fractional and fractal viscoelasticity. The D, KV and AZ models of viscoelasticity are considered due to the focus on time-dependent creep strain. Concrete creep, as with other mechanical properties of concrete materials [17, 18], is influenced by many parameters including compressive strength, mix proportions, elastic modulus, initial loading age, loading history and environmental conditions pre- and post-curing [19-21]. Herein, it is assumed that there is a perfect bond between the concrete and reinforcing and prestressing steel, and that the concrete is loaded in the service range (up to approx. $0.4f_c'$). Hence, the developed models are limited to linear concrete creep and do not consider the non-linear creep range. The fractional and fractal viscoelastic models will be compared for accuracy using existing experimental data in the literature and efficiency for both cases of constant and time-varying loading.

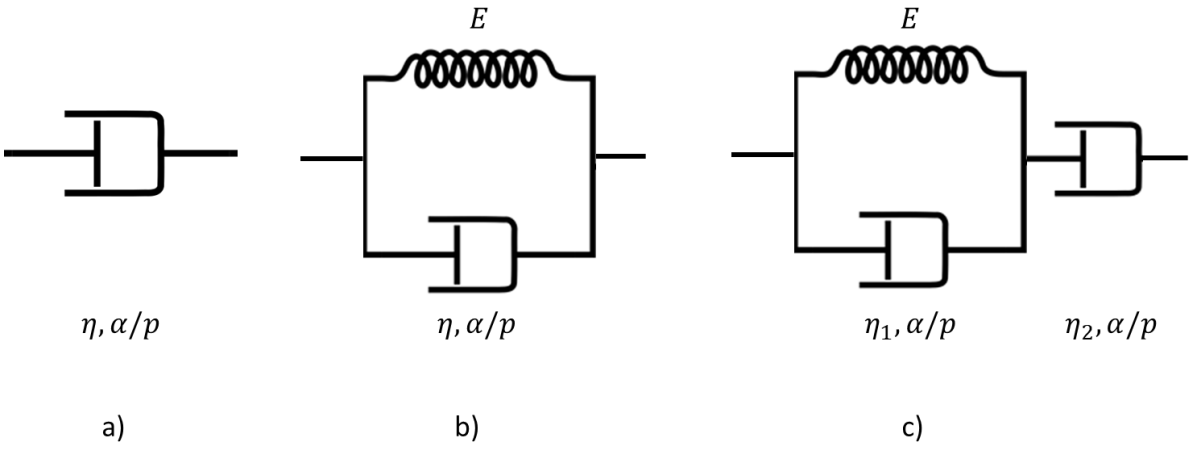

Figure 1 Dashpot (D), Kelvin-Voigt (KV) and anti-Zener (AZ) models of viscoelasticity

2 Model Development

2.1 Rheological model and equilibrium equations

The total strain in concrete is defined as;

$$\epsilon_c = e_{c,el} + e_{sh} + \epsilon_{cr} \tag{5}$$

where $e_{c,el}$ is the instantaneous mechanical strain, e_{sh} is the shrinkage strain, and ϵ_{cr} denotes the basic creep strain. Thermal expansion is ignored herein as the focus is concrete at constant ambient temperatures. Moreover, the concrete is assumed to be loaded in the elastic region and therefore, the mechanical strain does not incorporate inelastic deformations. To ensure strain compatibility between the concrete and steel reinforcing bars, the total concrete strain must equate to the strain in the reinforcing steel ϵ_s and prestressing steel ϵ_p. Hence,

$$\epsilon_c = \epsilon_s = \epsilon_p \tag{6}$$

Eqs. (5) and (6) are graphically represented in Fig. 2 as a rheological model consisting of the reinforcing steel, prestressing steel and concrete placed in parallel, with the concrete containing the mechanical, shrinkage and creeping elements placed in series. The equilibrium equation for a reinforced and prestressed concrete member subjected to concentric axial loading P is;

$$P = N_c + N_s + \Delta P \tag{7}$$

where N_c is the axial force in the concrete, N_S is the axial force in the reinforcing steel and ΔP is the loss of prestressing force. Combining Eqs. (5), (6) and (7) gives;

$$\frac{N_c}{A_c E_c} + \epsilon_{cr}(N_c) + \epsilon_{sh} = \frac{P - N_c}{A_s E_s + A_p E_p} \tag{8}$$

where $A_s$is the concrete cross-sectional area, E_c is the elastic modulus of concrete at the time of loading,A_s is the area of reinforcing steel, A_p is the area of prestressing steel, E_s is the elastic modulus of reinforcing steel and E_p is the elastic modulus of prestressing steel. Eq. (8) is then solved based on the selected viscoelastic model's constitutive stress-strain relation.

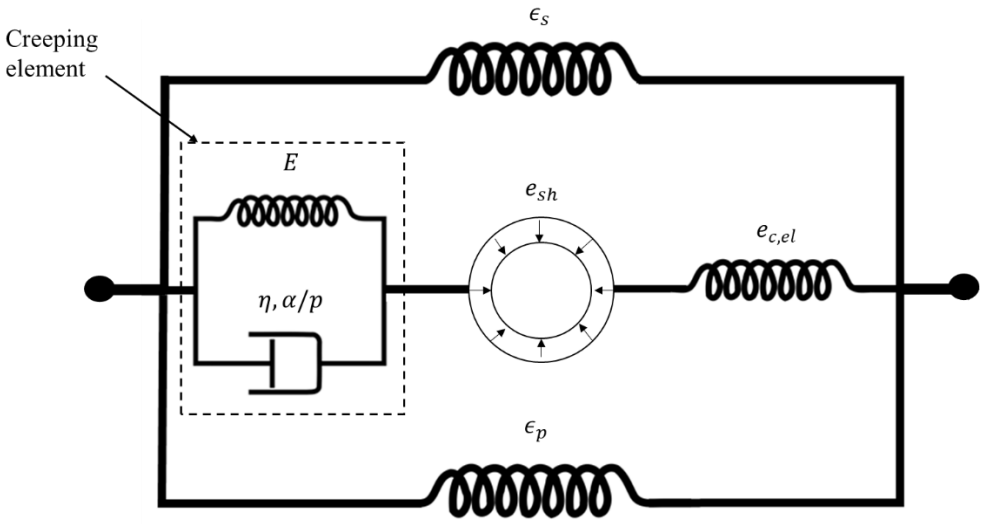

Figure 2 Rheological model of prestressed concrete consisting of reinforcing steel, prestressing steel and concrete elements in parallel.

2.2 Solutions for fractional viscoelastic models

If the applied axial loading is constant, and the shrinkage strain ignored, a semi-analytical expression for basic creep strain can be derived when adopting fractional viscoelastic constitutive laws. Substituting in the constitutive equation for the FKV model (Table 1) into Eq. (8) gives;

$$D_t^{\alpha}\,(\epsilon_{cr}) + c_1 \cdot \epsilon_{cr} - \; c_2 = 0 \tag{9}$$

where the constants c_1 and c_2 are;

$$c_1 = \frac{E}{\eta} + \frac{E_c(A_s E_s + A_p E_p)}{\eta\left(A_s E_s + A_p E_p + E_c A_c\right)}, \quad c_2 = \frac{P E_c}{\eta\left(A_s E_s + A_p E_p + E_c A_c\right)} \tag{10}$$

Applying the Laplace transform to Eq. (9) and rearranging yields;

$$\hat{\mathrm{E}}_{cr} = \left(\frac{c_2}{c_1}\right) \times \frac{c_1}{s\,(s^{\alpha} + c_1)} \tag{11}$$

where c_1 and c_2 denote constants. The basic creep strain is now derived using the inverse Laplace transform;

$$\epsilon_{cr} = \left(\frac{c_2}{c_1}\right) \times \mathcal{L}^{-1}\left[\frac{c_1}{s\,(s^{\alpha} + c_1)}\right] = \left(\frac{c_2}{c_1}\right)[1 - \mathcal{E}_{\alpha}(-c_1 t^{\alpha})] \tag{12}$$

In Eq. (12), $\mathcal{E}_{\alpha}$ is the Mittag-Leffler function;

$$\mathcal{E}_{\alpha}(x) = = \sum_{n=0}^{\infty} \frac{x^n}{\Gamma(\alpha n + 1)}\,. \tag{13}$$

For the case of non-constant loading and/or when the shrinkage strain is considered, numerical schemes must be employed to solve for the basic creep strain. The discretization approach derived by Bouras et al. [9] for the Caputo fractional derivative is adopted and generalized for the FKV model of viscoelasticity giving;

$$\epsilon_n = \frac{\epsilon_{n-1} - \sum_{j=0}^{n-2}\left(\epsilon_{j+1} - \epsilon_j\right)[(n-j)^{1-\alpha} - (n-j-1)^{1-\alpha}] + \frac{N_{c,n}}{A_c \eta}\,\Gamma\,(2-\alpha)(\Delta t)^{\alpha}}{\frac{E}{\eta}\,\Gamma\,(2-\alpha)\Delta t^{\alpha} + 1} \tag{14}$$

where Δt is the time step size, $t = n\Delta t, n = 2 \ldots t_f/\Delta t$, t_f is the final time, and $(\,')_n = (\,')\ (\mathrm{n}\Delta\mathrm{t})$. Derivation of Eq. (14) is shown in the Appendix. Creep strain at $n = 1$ is;

$$\epsilon_{cr,1} = \frac{\mathrm{N}_{c,1}\,\Gamma\,(2-\alpha)(\Delta t)^{\alpha}/(A_c \eta)}{E\,\Gamma(2-\alpha)\Delta t^{\alpha}/\eta} + \epsilon_{cr,0} \tag{15}$$

and $\epsilon_{cr,0} = 0$. Eqs. (8) and (14) are then solved simultaneously at every time step. Both semi-analytical solution (12) and numerical solution (14) can be reverted to the FD model by setting $E = 0$. If the shrinkage strain is ignored, numerical solution (14) and Eq. (8) give the same result. Only a minor difference in creep is observed if the shrinkage strain is considered in numerical procedure (14), see Fig. 3. Typically, a time-step size of $\Delta t = 1$ day is sufficient to provide accurate results.

2.3 Solutions for fractal viscoelastic models

When adopting fractal viscoelastic equations, closed-form solutions for basic creep in reinforced and prestressed concrete can be obtained if the loading is constant and shrinkage strain is ignored. Combining Eq. (8) with the stress-strain relation of the fractal KV viscoelastic model gives;

$$\frac{\dot{\epsilon_{cr}}}{p \cdot t^{p-1}} + c_1 \cdot \epsilon_{cr} - c_2 = 0 \tag{16}$$

Eq. (16) has the following solution which can be obtained using conventional means;

$$\epsilon_{cr} = \frac{c_2}{c_1}\left(1 - e^{-c_1 t^{p}}\right) \tag{17}$$

The fractal viscoelastic equations can be solved numerically using discretization approaches for the cases of non-constant loading and/or when the shrinkage strain is considered. Applying a backwards Euler scheme to the fractal KV model gives;

$$\epsilon_{cr,n} = \frac{N_{c,n} p \Delta t \, (n\Delta t)^{p-1} + A_c \eta \, \epsilon_{cr,n-1}}{A_c \eta + A_c E p \Delta t \, (n\Delta t)^{p-1}} \tag{18}$$

Eqs. (4) and (18) can be solved simultaneously at every time step. Again, analytical solution (17) and numerical solution (18) can be reverted to the fractal D model by setting $E = 0$, and numerical solution (18) and Eq. (17) gives a very close result when shrinkage strain is ignored. However, in contrast to the fractional viscoelastic models, a much smaller time-step is required for the numerical approximation (18) to converge to the analytical expression (17). In the example depicted in Fig. 3 a time step size of $\Delta t = 0.01$ days was required whereas the numerical approximation of the FKV model was accurate with $\Delta t = 1$ day. The smaller time-step size requirement results in longer computation times. A smaller time-step size may be required due to the lack of history dependence in the numerical approximation of the fractal derivative which is only dependent on the creep strain in the previous time step. Whereas in the numerical approximation of the fractional differential equations, the entire creep strain history appears in every iteration.

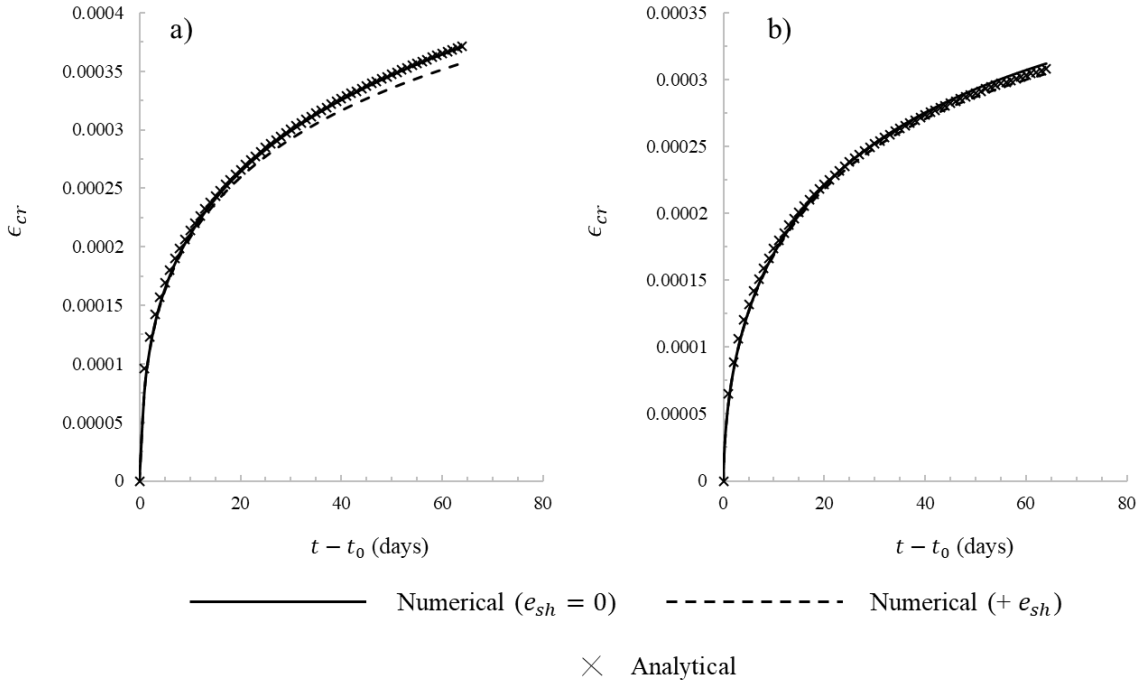

Figure 3 Comparison of analytical and numerical solutions for fractional (a) and fractal (b) models. $P = 842$ *kN,* $A_c = 5.8794 \times 10^4$*mm*^{4}*,* $A_s = 1.2064 \times 10^3$*,* $E_s = 2 \times 10^5$*MPa and* $e_{c,el} = 0.00034$*.* $\alpha = 0.4$*,* $\eta = 1.4129 \times 10^5$ *MPa·days*$^\alpha$*,* $E = 9.1838 \times 10^3$*MPa and* $\Delta t = 1$ *day (a).* $p = 0.504$*,* $\eta = 1.8269 \times 10^5$ *MPa·days,* $E = 2.7032 \times 10^4$*MPa and* $\Delta t = 0.01$ *days (b).*

3 Model Calibration

The dynamic viscosity η, elastic modulus E and fractional/fractal order α/p of the fractional and fractal viscoelastic models require calibration for specific concretes. This can be achieved by curve-fitting the associated creep compliances with experimental data of basic creep tests in plain concrete under constant stress. The Least-Squares Method (LSM) was adopted to obtain the model parameters using experimental results available in the literature. Studies were selected that conducted basic creep tests on plain concrete specimens followed by creep tests on reinforced or prestressed concrete, or creep tests with multi-stage loading, for verification of the developed

models in the proceeding sections. Table 2 lists the calibrated parameters in addition to the testing and concrete properties, and Fig. 4 depicts the fitted creep curves and experimental data. The FKV and fractal KV viscoelastic models lead to highly accurate representations of creep behavior in all cases examined. However, the FD and fractal D models could not accurately capture the creep strain behaviour in all cases, as seen in Fig. 4 (c) and (d). The dashpot models cannot reflect the decaying creep rate creep plateau after long time periods. Due to the sensitivity of the model parameters to the material characteristics of concrete and loading properties, the models require calibration before application in other scenarios not considered herein.

Table 2 Calibrated model parameters and creep test data

	Reference	[22]	[23]	[24]	[25] A	[25] B	[26]
	Fig. 4	a)	b)	c)	d)	e)	f)
	$f_c^{'}$ (MPa)	52.8	37.2	27.0	30.0	28.0	62.0
	σ / f_c'	0.400	0.310	0.424	0.167	0.179	0.400
	E_c (MPa)	46,600.0	28,150.0	23,714.7	29,400	22,700	42,000
	t_o (days)	14	28	15-20	10	7	28
FKV	$\eta \times e_{c,el}$ (MPa·day$^{\alpha}$)	121.268	40.654	224.494	58.726	12.416	2368.691
	$E \times e_{c,el}$ (MPa)	7.795	4.593	6.137	4.402	1.066	282.441
	α	0.400	0.400	0.966	0.816	0.572	0.371
FD	$\eta \times e_{c,el}$ (MPa·day$^{\alpha}$)	98.340	34.417	9.749	26.607	9.277	1940.298
	α	0.279	0.249	0.155	0.360	0.352	0.219
Fractal KV	$\eta \times e_{c,el}$ (MPa·day$^{\mathrm{p}}$)	149.710	37.929	264.451	52.032	10.893	1813.750
	$E \times e_{c,el}$ (MPa)	13.532	6.463	6.185	4.716	1.311	370.952
	p	0.485	0.401	1.000	0.778	0.547	0.323
Fractal D	$\eta \times e_{c,el}$ (MPa·day$^{\mathrm{p}}$)	81.016	31.209	9.081	23.685	8.265	1667.321
	p	0.263	0.249	0.155	0.360	0.352	0.208

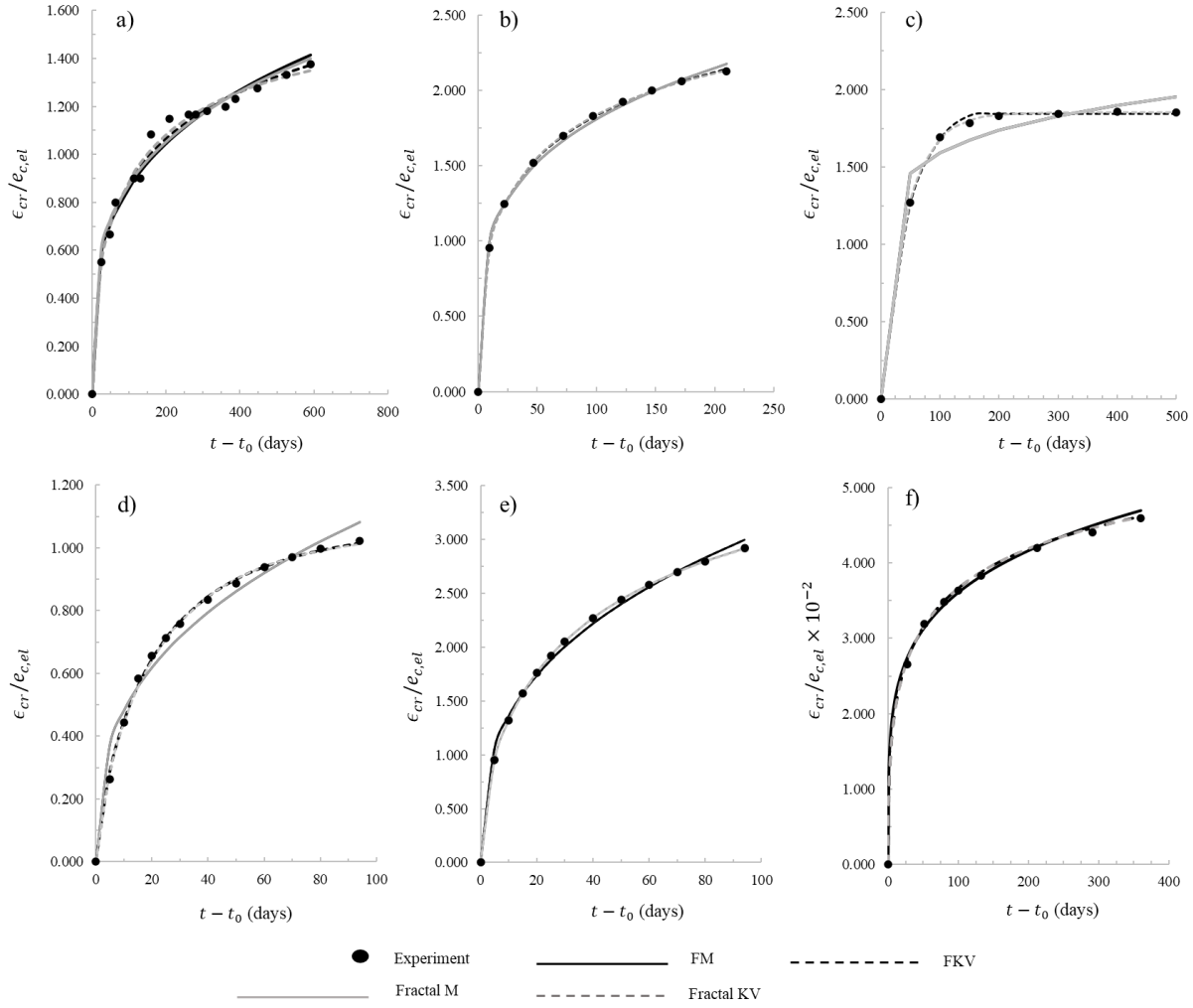

Figure 4 Fitting creep compliances of viscoelastic models to experimental data of basic creep in plain concrete

During creep testing it is possible for the applied loading to decrease with time due to the deformations of the test specimen. When stress relaxation is observed, the viscoelastic model parameters cannot be obtained by fitting the creep compliance to the test results as the compliance function is obtained by solving the constitutive stress-strain relations of the viscoelastic models under constant stress. Instead, the numerical approximations of the fractional differential Eq. (14) and fractal differential Eq. (18) must be fitted to the creep test data. Zhou et al. [26] measured creep in high-strength concrete whilst considering the stress relaxation effect. Three types of high-strength concrete mixtures were analysed with initial loading ages of $t_o = 7$ days and $t_o = 28$ days. The creep strain of one specimen is shown in Fig.4 (f) in addition to the fitted creep curves. The concrete properties and calibrated viscoelastic parameters are provided in Table 2, and the applied loading is depicted in Fig. 5 (a). A time step-size of $\Delta t = 1$ day was adopted to calibrate the fractional models. Smaller time-steps are required when calibrating the fractal equations, particularly for the fractal D model. The fractal KV and fractal D model parameters were determined with time step-size of $\Delta t = 0.01$ days and $\Delta t = 1 \times 10^{-5}$ days respectively. Hence, it is recommend that the parameters for the fractal D models be obtained through the FD model, as the fractional exponent α is equal to the fractal order p, and the dynamic viscosity in the fractal D model is equal to the dynamic viscosity in the FD model $\eta \times \Gamma(1 + \alpha)$. The FKV creep compliances obtained when the stress relaxation is considered and not considered are shown in Fig. 5 (b). In the case of the later, the stress is taken as

constant and equal to the initial applied stress $\sigma_0 = 25$ MPa. A noticeable difference is seen in the obtained creep compliances, emphasising the importance of consideration of stress relaxation which otherwise leads to an underestimation of creep strain.

4 Model Verification

4.1 Constant loading

Analytical expressions (12) and (17) are now verified by comparison to experimental results available in the literature. Short-term creep tests on prestressed concrete under sustained loading were conducted by Pan et al. [22] for three different reinforcement ratios. The viscoelastic model parameters listed in Table 2 were obtained using the creep tests conducted on plain concrete cubes featuring a size of 100×100×30 mm. As the prestressed concrete specimens measured at 250 × 250 mm, a creep correction factor for specimen size was applied to the viscoelastic model parameters η and E using the ACI 209R-92 method [27]. The size correction factor $\gamma_{VS} = 2/3[1 + 1.13e^{-0.0213\,VS}]$ where VS is the volume-to-surface ratio, in this case 62.5 mm. The size factor was considered by dividing E and η by γ_{VS}. Area A_p and elastic modulus E_p of prestressing steel was taken as 808.175 mm^2 and 205,000 MPa respectively. Fig. 6 shows the results alongside the analytical Eqs. (12) and (17). The Kelvin-Voigt models show a high level of agreement with the experimental data for the 0.38% and 0.76% reinforcement ratios, and slightly over predict creep in the 1.71% reinforcement ratio case. The Maxwell models lead to higher creep strains in all three cases.

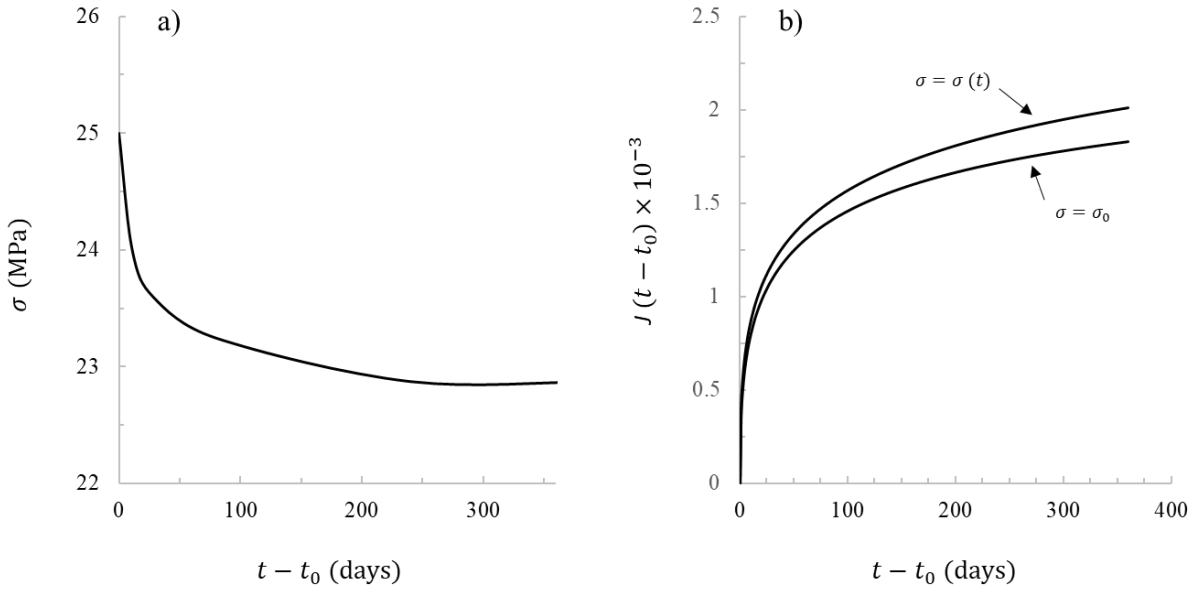

Figure 5 Relaxation of applied loading in creep tests in [26] a) and FKV creep compliances obtained with and without consideration of stress relaxation b).

4.2 Time-varying loading

Zou et al. [23] conducted creep tests on plain 100 × 100 mm rectangular concrete specimens subjected to multi-stage loading. Axial loading was increased by 6 kN every 3, 5 or 7 days until the maximum loading of 180 kN was reached. The first load was applied at 6 days and the total duration of the tests was 230 days. Two specimens were cast for each loading scenario and the observed

creep strains were averaged. Fig. 7 depicts the stress-induced axial strains ($e_{c,el} + \epsilon_{cr}$) observed in the experiments and the predictions of the derived numerical models. It is shown that the FKV model leads to a highly accurate representation of axial strain for the case of time-varying loading. The results of the FM model are indistinguishable to FKV model and have been omitted from Fig. 7 for clarity Conversely, the fractal derivative-based models are greatly inaccurate and significantly underestimate creep strain for cases of time-varying loading. The 28-day elastic modulus of 28,150 MPa was taken as $\mathrm{E_c}$ and a time step size of $\Delta t = 1$ day was adopted for the numerical procedures. Smaller time steps were not found to not noticeably influence results for the fractional models but led to longer computation times. It is possible that the accuracies of the fractal models can be increased through construction of a fractal M or KV chain, however; as discussed previously, calibration of model parameters then becomes convoluted and the advantages associated with fractal models diminish.

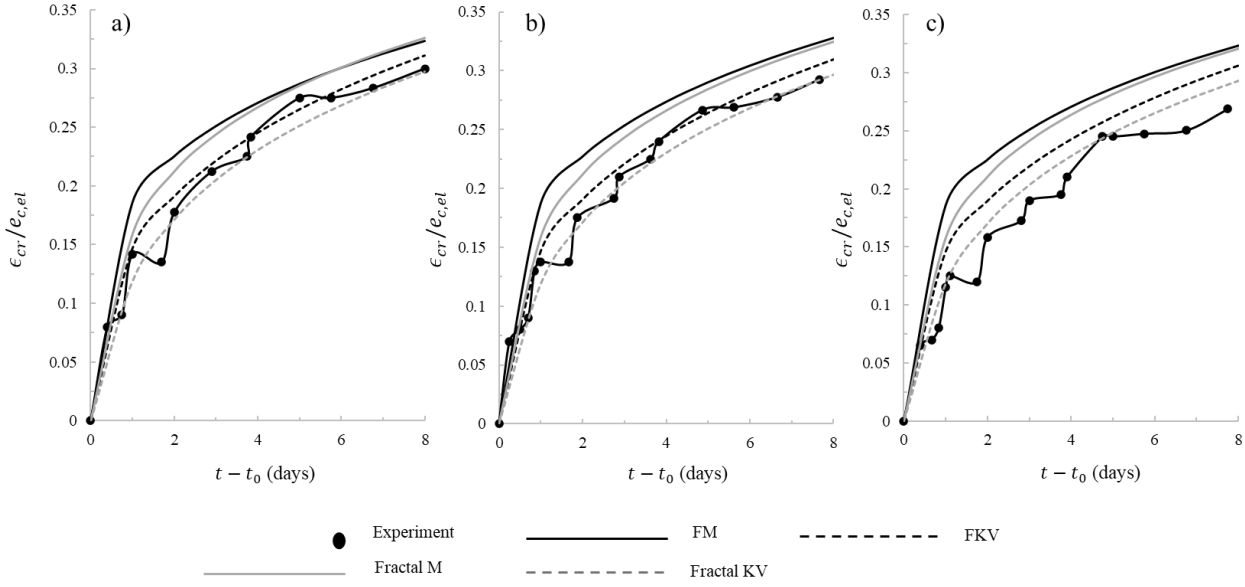

Figure 6 Comparisons of experimental results and analytical equations for creep strain in pre-stressed concrete at 0.38% (a), 0.76% (b) and 1.71% (c) reinforcement ratios.

The numerical approximations of the fractional and fractal derivative models are also compared to the experimental results presented by Park et al. [25], who conducted creep tests on plain concrete under sustained and multi-stage loading. The cylindrical concrete specimens featured a diameter of 150 mm and a height of 300 mm and were loaded at 10 days (Specimen A) and 7 days (Specimen B). The model parameters for both specimens were calibrated using the sustained loading tests depicted in Fig. 4 and are listed in Table 2. It can be seen that initial loading age significantly influences the model parameters. Comparisons between the derived numerical methods and the experimental results for stepwise loading scenarios are shown in Fig. 8. Four specimens were tested for each loading scenario and the measured creep strains were averaged. The FM and FKV models are accurate though slightly over predict the creep strain by less then 10%. The fractal M model leads to a significant underestimation of creep strain whereas the fractal KV model is accurate for Specimen A and underestimates creep in Specimen B. Additionally, Fig. 8 shows the predictions based on the Parallel curve method proposed by Park et al. [25] and the age-adjusted effective modulus (AAEM) method for comparison to the fractional and fractal models. The Parallel curve addresses the significant underestimation of creep by the rate of creep (RCM) method when concrete is subjected to step-loading. In the RCM method, creep curves due to loading at different ages feature the same tangent at given point in time i.e., the curves are vertically parallel and creep

rate is independent of loading age. The Parallel curve method combines the RCM method with a horizontal parallel curve assumption (tangent of curves is constant along a horizontal line) and relates them through an ageing parameter. Effectively, the Parallel curve method bounds the actual creep between a horizontal parallel assumption (upper limit) and the vertical parallel assumption (lower limit). Creep strain at time t_n due to loading at $t_0, t_1, t_2 \ldots\ldots t_{n-1}$ is defined using the Parallel curve method as;

$$\epsilon_{cr}(t_n) = [1 - \alpha_x(t_n)] \sum_{i=1}^{n} [J'(t_n, t_0) - J'(t_{i-1}, t_0)] \Delta\sigma_{i-1} + \alpha_x(t_n) \sum_{i=1}^{n} [J'(t_n - t_{i-1} + t_0, t_0)] \Delta\sigma_{i-1} \quad (19)$$

Where $\Delta\sigma_{i-1}$ is the stress increment at t_{i-1} and α_x is the ageing factor. The AAEM method is defined as;

$$\epsilon_{cr}(t_n) = \sigma_c(t_o)\, J(t_n, t_0) + \Delta\sigma_c(t_n)\, \chi(t_n, t_0)\, J(t_n, t_0) \quad (20)$$

where $\Delta\sigma_c(t_n)$ is the change in stress level from t_0 to t_n and $\chi(t_n, t_0)$ is the stress-dependent ageing coefficient. As the Parallel curve and AAEM methods are dependent on an existing creep compliance $J(t, t_0)$, for comparison to the models derived herein the fractal KV model's creep compliance was adopted with the parameters provided in Table 2. The Parallel curve method is highly accurate and selection of different fractional and fractal creep compliance equations $J(t, t_0)$ from Table 1 had a negligible influence on results. The AAEM method is not as accurate as the Parallel curve method. When compared to the fractional M and KV models, the AAEM method is not as accurate during majority of the creep test, particularly when loading is applied, however converges to the experimental results towards the end of the testing period. Aging factors of $\alpha_x = 0.75$ and $\chi(t_n, t_0) = 0.8$ were recommended by Park et al. [25] and were adopted for the predictions shown in Fig. 8. The Parallel curve and AAEM methods were also compared with the experiments conducted by Zou et al. [23], see Fig. 9 and 10. In this case, the aging factors α_x and $\chi(t_n, t_0)$ required recalibration and best results were obtained when $\alpha_x = 1.0$, 0.90 and 0.85 and $\chi(t_n, t_0)$ = 1.0, 0.9 and 0.8 for the 3-, 5- and 7-day loading tests respectively. This result highlights the increasing effects of ageing with loading period. In this case, the FM and FKV models give indistinguishable results to the Parallel curve method with $\alpha_x = 1.0$. Hence, the Parallel curve method can yield more accurate results then the FM and FKV models for concrete subjected to time-varying loading due to the consideration of aging. However, the aging factor α_x requires calibration using creep test data specific to the loading history in question. Incorporation of ageing effects into the FM and FKV models for prediction of concrete creep will be considered in future research works.

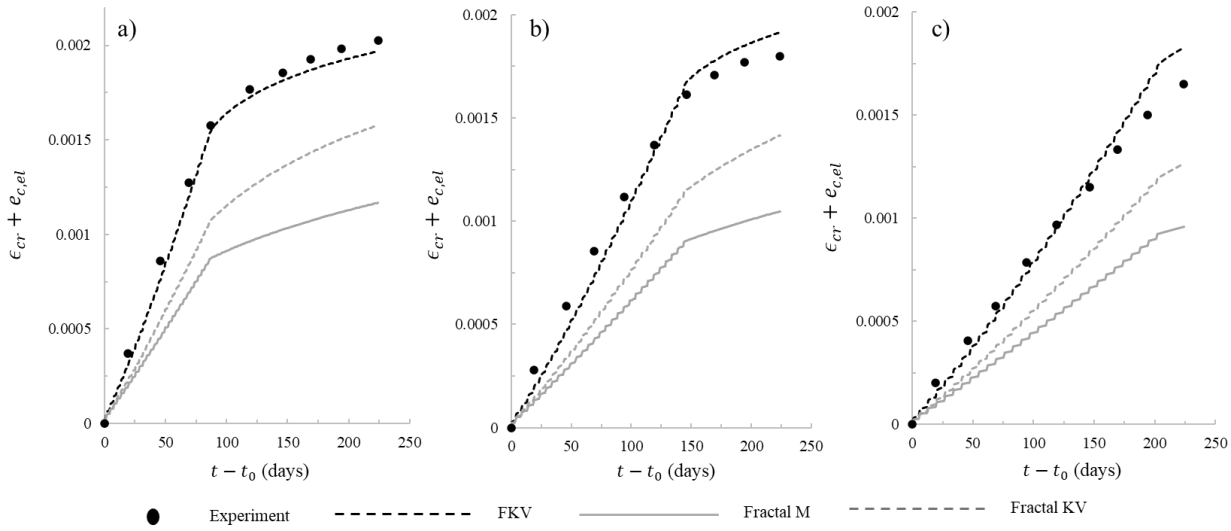

Figure 7 Comparisons of experimental results and numerical models for stress-induced axial strain in plain concrete under multi-stage loading at 3-day (a), 5-day (b) and 7-day (c) intervals.

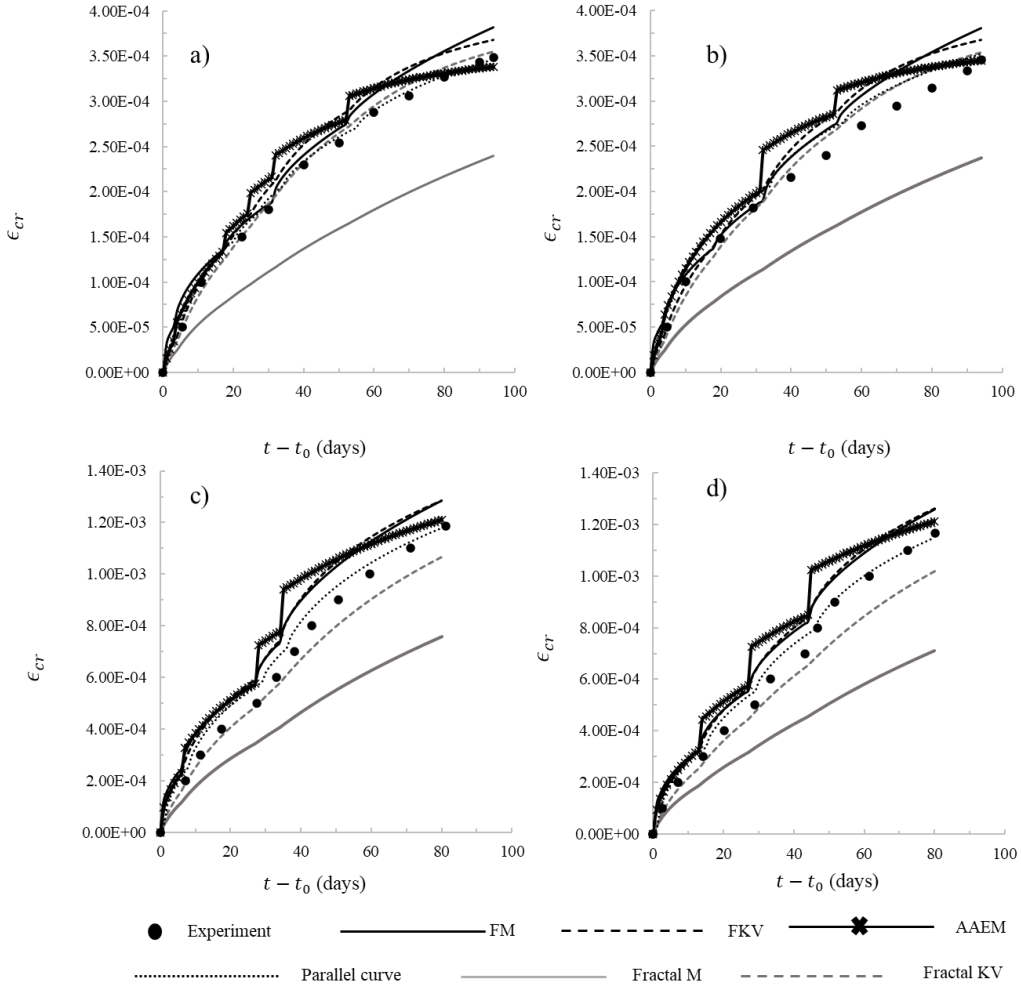

Figure 8 Comparisons of experimental results from [25] and numerical models for creep strain in plain concrete under piecewise multi-stage loading. Specimen A load case 1 (a), specimen A load case 2 (b), specimen B load case 1 (c) and specimen B load case 2 (d).

5 Conclusions

A rheological model for determining linear creep in reinforced and prestressed concrete under constant and time-varying loads was developed in this paper based on fractional and fractal viscoelastic laws. The parameters of the Dashpot and Kelvin-Voigt models were calibrated by fitting creep compliances with existing experimental data on basic creep in plain concrete. The viscoelastic models allowed an accurate representation of basic creep with only few model parameters. Analytical expressions were derived for creep in reinforced and prestressed concrete under constant loading by solving the resulting fractional and fractal differential equations. Comparisons the closed-from solutions and experimental show a high - level of agreement for the Kelvin-Voigt based models, with the Dashpot models overpredicting creep strain. For the case of time-varying loading, numerical procedures were employed to determine creep strain. The fractional derivative-based models were shown to predict creep accurately and efficiently in plain concrete under multi-stage loading, whereas the fractal-based models significantly underpredicted creep. Overall, the fractional KV model proved to be the most accurate and robust method to model creep in concrete. Future research areas include relating the viscoelastic model parameters to physical properties of concrete, generalising the models for non-linear creep, further consideration of ageing effects and investigating the influence of temperature and humidity on model parameters. Different approaches to numerically solving fractional and fractal differential equations, including those that allow variable time steps to be employed, can also be explored.

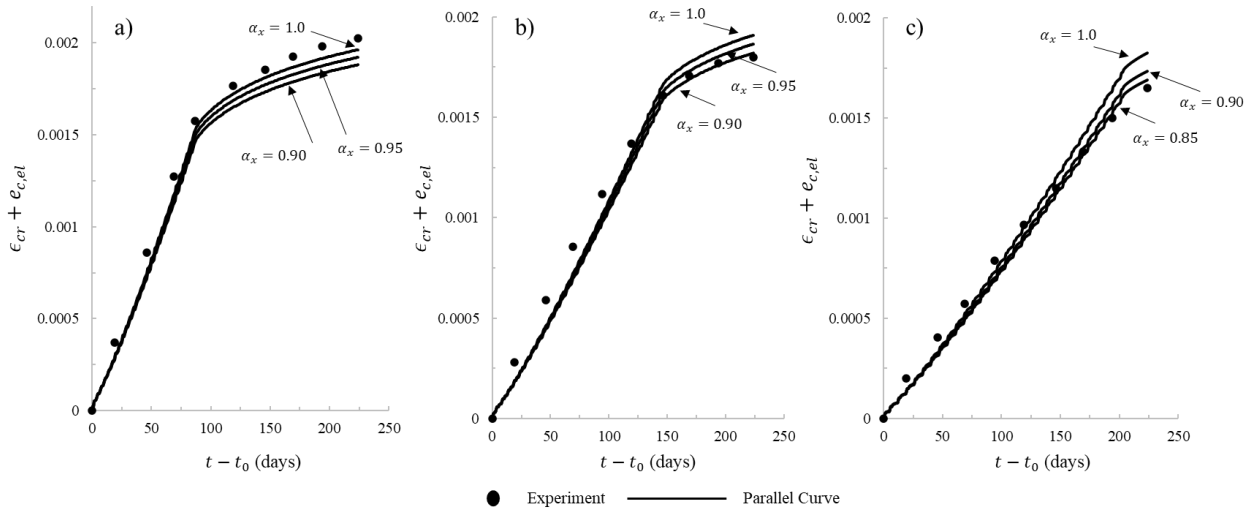

Figure 9 Effect of ageing factor α_x on accuracy of Parallel curve method when compared to experimental results by [23] for stress-induced axial strain in plain concrete under multi-stage loading at 3-day (a), 5-day (b) and 7-day (c) intervals.

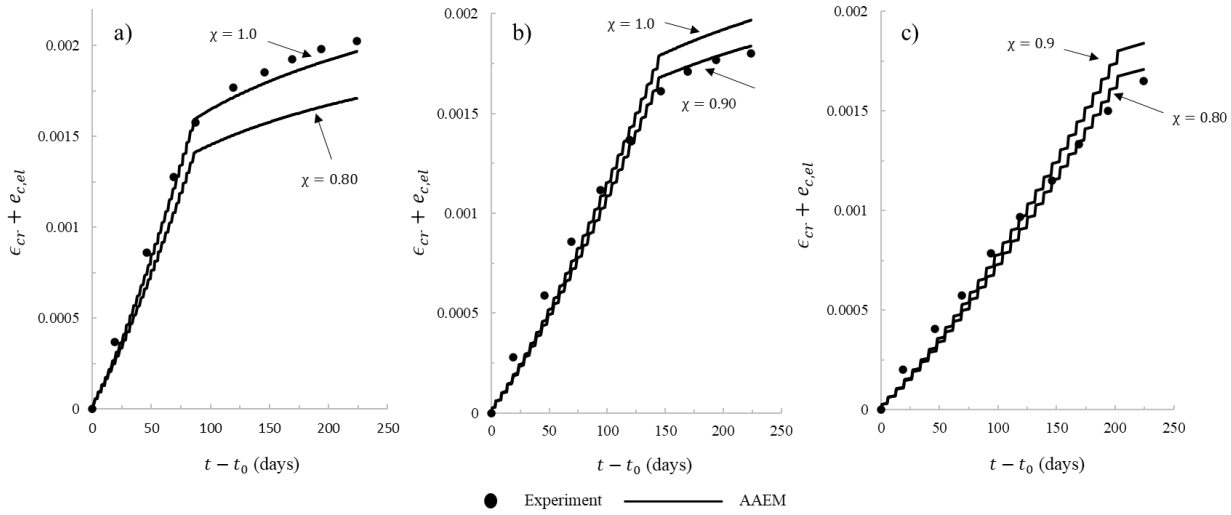

Figure 10 Effect of ageing factor χ accuracy of AAEM method when compared to experimental results by [23] for stress-induced axial strain in plain concrete under multi-stage loading at 3-day (a), 5-day (b) and 7-day (c) intervals.

Appendix

The Caputo fractional derivative is discretised as follows;

$$D_t^{\alpha} f(t) = \frac{1}{\Gamma(1-\alpha)} \int_0^t \frac{D_t^1 f(\tau)}{(t-\tau)^{\alpha}}\, d\tau. \tag{21}$$

$$\approx D_t^{\alpha} f(t) = \frac{1}{\Gamma(1-\alpha)} \sum_{j=0}^{n-1} \int_{j\Delta t}^{(j+1)\Delta t} \frac{D_t^1 f(\tau)}{(t-\tau)^{\alpha}}\, d\tau. \tag{22}$$

$$\approx D_t^{\alpha} f(t) = \frac{1}{\Gamma(1-\alpha)} \sum_{j=0}^{n-1} \int_{j\Delta t}^{(j+1)\Delta t} \frac{f_{j+1} - f_j}{\Delta t\,(t-\tau)^{\alpha}}\, d\tau. \tag{23}$$

$$\approx D_t^{\alpha} f(t) = \frac{1}{\Gamma(1-\alpha)\Delta t^{\alpha}} \sum_{j=0}^{n-1} (f_{j+1} - f_j)[(n-j)^{1-\alpha} - (n-j-1)^{1-\alpha}]\ . \tag{24}$$

$$\approx D_t^{\alpha} f(t) = \frac{1}{\Gamma(2-\alpha)\Delta t^{\alpha}} \sum_{j=0}^{n-1} (f_{j+1} - f_j)[(n-j)^{1-\alpha} - (n-j-1)^{1-\alpha}]\ . \tag{25}$$

$$\approx D_t^{\alpha} f(t) = \frac{1}{\Gamma(2-\alpha)\Delta t^{\alpha}} \sum_{j=0}^{n-2} (f_{j+1} - f_j)[(n-j)^{1-\alpha} - (n-j-1)^{1-\alpha}] + \frac{f_n - f_{n-1}}{\Gamma\,(2-\alpha)\Delta t^{\alpha}}. \tag{25}$$

The following creep strain ϵ_{cr} for the FKV model is obtained by substituting Eq. (24) into the stress-strain relation;

$$\epsilon_{cr,n} = \frac{\frac{\sigma_n}{\eta}\Gamma\,(2-\alpha)\Delta t^{\alpha} + \epsilon_{cr,n-1} - \sum_{j=0}^{n-2}(\epsilon_{j+1}-\epsilon_j)[(n-j)^{1-\alpha} - (n-j-1)^{1-\alpha}]}{1+\frac{E}{\eta}\,\Gamma\,(2-\alpha)\Delta t^{\alpha}}, (26)$$

with ϵ_{cr} at time step $n = 1$derived as

$$\epsilon_{cr}\,(1) = \frac{\sigma_1\Gamma(2-\alpha)\Delta t^{\alpha}/\eta}{E\,\Gamma(2-\alpha)\Delta t^{\alpha}/\eta + 1} + \epsilon_{cr}(0)$$

and $\epsilon_{cr}(0) = 0$.

References

1. Pritz, T., *Analysis of four-parameter fractional derivative model of real solid materials.* Journal of Sound Vibration, 1996. **195**(1): p. 103-115.
2. Bazant, Z.P. and L. Cedolin, *Stability of structures: elastic, inelastic, fracture and damage theories*. 2010: World Scientific.
3. Bonfanti, A., et al., *Fractional viscoelastic models for power-law materials.* Soft Matter, 2020. **16**(26): p. 6002-6020.
4. Hilfer, R., *Applications of fractional calculus in physics*. 2000: World scientific.
5. Liu, J., et al., *A four-element fractional creep model of weakly cemented soft rock.* Bulletin of Engineering Geology and the Environment, 2020. **79**(10): p. 5569-5584.
6. Liu, X., et al., *A Caputo variable-order fractional damage creep model for sandstone considering effect of relaxation time.* Acta Geotechnica, 2021: p. 1-15.
7. Wu, F., et al., *New fractional variable-order creep model with short memory.* Applied Mathematics and Computation, 2020. **380**: p. 125278.
8. Xu, X.-B. and Z.-D. Cui, *Investigation of a fractional derivative creep model of clay and its numerical implementation.* Computers and Geotechnics, 2020. **119**: p. 103387.
9. Bouras, Y., et al., *A non-linear thermo-viscoelastic rheological model based on fractional derivatives for high temperature creep in concrete.* Applied Mathematical Modelling, 2018. **55**: p. 551-568.
10. Di Paola, M. and M.F. Granata, *Fractional model of concrete hereditary viscoelastic behaviour.* Archive of Applied Mechanics, 2017. **87**(2): p. 335-348.
11. Beltempo, A., et al., *A fractional-order model for aging materials: An application to concrete.* International Journal of Solids and Structures, 2018. **138**: p. 13-23.
12. Zhang, C., et al., *Nonlinear creep damage constitutive model of concrete based on fractional calculus theory.* Materials, 2019. **12**(9): p. 1505.
13. Bagley, R.L. and P.J. Torvik, *On the fractional calculus model of viscoelastic behavior.* Journal of Rheology, 1986. **30**(1): p. 133-155.
14. Cai, W., W. Chen, and W. Xu, *Characterizing the creep of viscoelastic materials by fractal derivative models.* International Journal of Non-Linear Mechanics, 2016. **87**: p. 58-63.
15. Wang, R., et al., *A fractal derivative constitutive model for three stages in granite creep.* Results in Physics, 2017. **7**: p. 2632-2638.
16. Qu, P., X. Liu, and D. Baleanu, *Simulating chloride penetration in fly ash concrete by a fractal derivative model.* Thermal Science, 2019. **23**(Suppl. 1): p. 67-78.
17. Wu, J., et al., *Particle size distribution of aggregate effects on mechanical and structural properties of cemented rockfill: experiments and modeling.* Construction and Building Materials, 2018. **193**: p. 295-311.
18. Wu, J., et al., *Effects of carbon nanotube dosage and aggregate size distribution on mechanical property and microstructure of cemented rockfill.* Cement and Concrete Composites, 2022. **127**: p. 104408.
19. Bazant, Z.P. and J.J.M. Chern, *Concrete creep at variable humidity: constitutive law and mechanism.* Materials and structures, 1985. **18**(1): p. 1-20.
20. Bažant, Z.P., et al., *Microprestress-solidification theory for concrete creep. I: Aging and drying effects.* Journal of engineering mechanics, 1997. **123**(11): p. 1188-1194.
21. Sellier, A., et al., *Concrete creep modelling for structural applications: non-linearity, multi-axiality, hydration, temperature and drying effects.* Cement and Concrete Research, 2016. **79**: p. 301-315.
22. Pan, Z., Z. Lü, and C.C. Fu, *Experimental study on creep and shrinkage of high-strength plain concrete and reinforced concrete.* Advances in Structural Engineering, 2011. **14**(2): p. 235-247.
23. Zou, D., et al., *Time-dependent deformations of concrete columns under different construction load histories.* Advances in Structural Engineering, 2019. **22**(8): p. 1845-1854.
24. Shariff, M.N., U. Saravanan, and D. Menon, *Time-dependent strains in axially loaded reinforced concrete columns.* Journal of Engineering Mechanics, 2020. **146**(8): p. 04020076.

25. Park, Y.-S., Y.-H. Lee, and Y. Lee, *Description of concrete creep under time-varying stress using parallel creep curve.* Advances in Materials Science and Engineering, 2016. **2016**.
26. Zhou, Y., W. Chen, and P.J.J.o.B.E. Yan, *Measurement and modeling of creep property of high-strength concrete considering stress relaxation effect.* 2022: p. 104726.
27. ACI, *ACI PRC-209-92: Prediction of Creep, Shrinkage, and Temperature Effects in Concrete Structures*. 2002, American Concrete Institute.